Hans-Jürgen von Martens
Physikalisch-Technische Bundesanstalt (PTB)
Fürstenwalder Damm 388
12587 Berlin, Germany

Investigations into the Uncertainties of Interferometric Measurements of Linear and Circular Vibrations

A uniform description is given of a method of measurement using a Michelson interferometer for measuring the linear motion quantities acceleration, velocity and displacement, and a diffraction grating interferometer for measuring the circular motion quantities angular acceleration, angular velocity and rotation angle. The paper focusses on an analysis of the dynamic behaviour of an interferometric measurement system based on the counting technique with regard to the measurement errors due to deterministic and stochastic disturbing quantities. The error analysis and description presented are aimed at giving some rules, mathematical expressions and graphical presentations that have proved to be helpful in recognizing the errors in interferometric measurements of motion quantities, optimizing the measurement conditions (e.g., filter settings), obtaining corrections and estimating the uncertainty of measurement.

INTRODUCTION

The manufacturers and users of vibration and shock measuring instrumentation are increasingly required to establish and ensure traceability to a national standard that represents the respective physical quantity. The common terms vibration and (mechanical) shock are defined as special variations with time of a physical quantity which is descriptive of the motion or excitation of a mechanical system. The quantities whose realization and dissemination are extensively required for establishing traceability are the linear motion quantities acceleration, velocity and displacement, and the circular motion quantities angular acceleration, angular velocity and rotation angle. To achieve the required level of traceability, the calibrations of reference or working standards (e.g., a reference standard accelerometer) and the tests of ordinary measuring instruments must be carried out with time variations that are relevant to the conditions of application (e.g., sinusoidal vibration or shock-shaped acceleration), and with sufficient accuracy to be expressed by the uncertainty of measurement.

Note. *The measurement uncertainty is understood in this article as the expanded uncertainty (coverage factor 2) defined by the Guide to the Expression of Uncertainty in Measurement (ISO, 1993) which represents an international convention (Taylor and Kuyatt, 1993).*

Received 20 December 1994; Revised 11 June 1997.
Shock and Vibration, Vol. 4, No. 5,6, pp. 327–340 (1997)
ISSN 1070-9622/97/$8.00 © 1997 IOS Press

Several national laboratories such as NIST currently provide, among other calibration services, steady-state sinusoidal calibration of pick-ups by laser interferometry using the methods stated in ISO 5347/0 (1997) and 5347/1 (1993) (Harris and Crede, 1987). The calibration shall be carried out by measuring displacement amplitude and frequency. To measure the displacement amplitude, the ISO standards specify the "fringe-counting method" (counting of the zero crossings of the Michelson interferometer signal) in the frequency range from 20 to 800 Hz, and the "minimum-point method" (adjusting the vibration to a level which makes the nth harmonic component zero) at frequencies from 800 to 5000 Hz.

Both methods have proved in various accelerometer round robins to be the most accurate calibration methods. In particular, the worldwide round robin organized and reported by Serbyn (1990) revealed, among other things, that the state of the art in application of the fringe counting method allows a measurement uncertainty of 0.1% to be achieved in acceleration amplitude measurements and accelerometer calibrations at middle frequencies (reference conditions: frequency 160 Hz and acceleration amplitude 10 m/s^2). The corresponding displacement amplitude of about 10 μm is usually seen as the lower displacement limit measurable with the conventional fringe-counting method because its amplitude measurement error can run up to $\lambda/4$ (wavelength $\lambda = 632.8$ nm for a He–Ne laser). However, to the surprise of some experts, the round robin mentioned above demonstrated the applicability of the counting method – in a modified version presented by Von Martens (1987) – over a widely extended frequency range from 0.5 Hz to 20 kHz at displacement amplitudes ranging from 0.5 m down to 5 nm.

The powerful capabilities of the fringe-counting method have been recognized and exploited by the author because of the well-known drawbacks of the minimum-point method (e.g., variation of the acceleration level in the measurement of accelerometer sensitivity as a function of frequency).

A hierarchy scheme for realizing and disseminating the unit of the physical quantity of acceleration, based on two-beam interferometry and counting technique has been presented by Von Martens and Rogazewski (1987).

In recent years at the PTB, the measurement method based on two-beam interferometry and the counting technique has been further developed allowing both linear and circular motion quantities to be measured with sinusoidal and other time dependences, such as shock-shaped accelerations and angular accelerations. A uniform description of the uniform method covering a variety of six motion quantities and various time dependences is given by Von Martens and Täubner (1994). Using the novel diffraction grating interferometer developed for measuring circular motion quantities, the (modified) fringe-counting method is being applied to rotation angle amplitudes from 10^{-7} to more than 10 rad.

The evaluation and expression of the measurement uncertainty to be stated for measurement and calibration results obtained with these methods for measuring linear and circular motion quantities may be viewed from two different aspects. One of them is the propagation of errors and uncertainties from the interferometrically measured characteristic (e.g., acceleration amplitude) to the calibration result (e.g., sensitivity or phase lag of an accelerometer). The error and uncertainty propagation demonstrated by Von Martens and Rogazewski (1987) for the hierarchy scheme presented there is considered relevant in this context. The other aspect is the evaluation of the individual error components in the interferometric measurements, due to the dynamic behaviour of the interferometer in conjunction with the photoelectric measuring chain under the influence of disturbing quantities. The investigation of this aspect is the subject of this article. Because of the complexity of an uncertainty description covering various time dependences this article focusses on the special case of sinusoidal motion quantities with no or low nonlinear distortions.

In the next section a brief description of the interferometric method of measuring both linear and circular motion quantities is given. The concept of the evaluation of the error and uncertainty components is outlined in the following section. The section further below describes and discusses the error and uncertainty components due to the dynamic behaviour of the interferometer in conjunction with the photoelectric measuring chain. Some applications are characterized and conclusions drawn in the final section.

MOTION QUANTITY MEASUREMENT BY TWO-BEAM INTERFEROMETRY

To measure the linear and circular motion quantities, two-beam interferometry has been applied making use of a single-frequency laser, a beam splitter, two reflectors (reflective sine phase gratings, if need be) and a single photoreceiver (cf. Figs. 10–13). The light beam emitted by the laser is split into two beams. After having been reflected (and, if need be, diffracted), these two beams are superimposed with the optical arrangement. This yields a light intensity whose significant component after photoelectric transformation can be

expressed by the relationship

$$u(t) = \hat{u} \cos \varphi(t), \tag{1}$$

where u is the interferometer signal (electric voltage) and $\hat{u}$ its amplitude. The total phase of the interferometer signal is

$$\varphi(t) = \varphi_M(t) + \varphi_0(t) + \varphi_C(t), \tag{2}$$

where φ_M is the phase term being proportional to the measurand, φ_0 is a simulated zero phase (cf. subsection entitled *Error due to quantization*) and φ_C is a frequency-converting phase which can be optionally used (Von Martens, 1993). The phase term φ_M in Eq. (2) can generally be expressed by

$$\varphi_M(t) = 2\pi \frac{s(t)}{\Delta s}. \tag{3}$$

In this relationship, $s(t)$ is the displacement sensed by the interferometer and Δs its quantization interval. The latter is $\lambda/2$ in the case of a Michelson interferometer. In the case of the diffraction grating interferometer described by Von Martens and Täubner (1994), the expression

$$\varphi_M(t) = 2\pi \frac{\Phi(t)}{\Delta\Phi}, \qquad \Delta\Phi = \frac{2\pi}{N_{360°}}, \tag{4}$$

can be obtained from Eq. (3). $\Phi(t)$ is the rotation angle to be measured, $\Delta\Phi$ the angle quantization interval corresponding to one interferometer signal period and $N_{360°}$ the total number of signal periods (impulses) counted while in an interferometer calibration mode, the moving part rotates a full 360° ($N_{360°} = 1.5 \times 10^6$, corresponding to $\Delta\Phi = 0.864$ arcsec in the version with a holographically manufactured circular sine phase grating used by the author). To give a uniform description covering both linear and circular motion, both the displacement s and the rotation angle Φ will be denoted by the "deflection" x, and the quantization intervals Δs and $\Delta\Phi$ by Δx. Thus, Eqs. (3) and (4) are uniformly expressed by

$$\varphi_M(t) = 2\pi \frac{x(t)}{\Delta x}. \tag{5}$$

The interferometer signal processing method introduced for measuring linear and circular motion quantities as is described by Von Martens and Täubner (1994), is based on identifying the signal zero crossings as "marks" of the deflection. By counting the zero crossings and measuring the time intervals between them, measurement points of the deflection–time relation can be determined. From the measurement results of the deflection x, the velocity or angular velocity is obtained by derivation

$$\dot{x}(t) = \frac{\mathrm{d}x}{\mathrm{d}t}, \tag{6}$$

and the acceleration or angular acceleration by double derivation

$$\ddot{x}(t) = \frac{\mathrm{d}^2x}{\mathrm{d}t^2}. \tag{7}$$

Special methods and algorithms leading, in the case of non-sinusoidal motion, from the measurement points x_i, t_i to the derivatives $\dot{x}(t)$ or $\ddot{x}(t)$ have been presented by Von Martens and Täubner (1994).

In the special case of sinusoidal time dependence,

$$x(t) = \hat{x} \cos(\omega t + \varphi_x), \tag{8}$$

with $\omega = 2\pi f_M$, the following expressions result from Eqs. (6) and (7):

$$\dot{x}(t) = \hat{\dot{x}} \cos(\omega t + \varphi_{\dot{x}}), \tag{9}$$

with $\hat{\dot{x}} = \omega\hat{x}$, $\varphi_{\dot{x}} = \varphi_x + \pi/2$, and

$$\ddot{x}(t) = \hat{\ddot{x}} \cos(\omega t + \varphi_{\ddot{x}}), \tag{10}$$

with $\hat{\ddot{x}} = \omega^2\hat{x}$, $\varphi_{\ddot{x}} = \varphi_x + \pi$. In these relationships, $\hat{x}$ is the amplitude of x, φ_x the zero-phase angle of x and f_M the frequency of the measurand.

If the vibration is sinusoidal, the continuous time interval measurement can be dispensed with because there is a priori information on the time dependence. Time measurement can be restricted to discrete parameters such as period duration or frequency. As is known from the conventional fringe counting method stated in ISO 5347/0 (1987) and ISO 5347/1 (1993), the amplitude of the displacement or rotation angle can be obtained through the relation

$$\hat{x} = \frac{N}{4M}\Delta x, \tag{11}$$

where N is the number of zero crossings counted during M vibration periods.

MEASUREMENT ERROR TREATMENT AND UNCERTAINTY ESTIMATION

The dynamic behaviour of the interferometer, when influenced by significant disturbing quantities, has

been investigated in conjunction with the Doppler signal processing subsystem. The part of this subsystem which is of particular interest is the photo-electric measuring chain that basically consists of a photoreceiver with a signal conditioner (including amplifier), a filter and a counter with a trigger. The interferometer can be described as a phase-analogous system which transforms a deflection into a proportional phase variation of the light intensity that illuminates the photoreceiver. The photoreceiver (if appropriately selected), the signal conditioner and the filter can be considered in terms of systems theory, linear systems described by their frequency characteristics (amplitude and phase characteristics). The counter with its trigger is a nonlinear system whose trigger level and trigger hysteresis are significant characteristics.

In principle, a signal-processing method which is based on the counting of the zero crossings of the interferometer signal is sensitive to stochastic and deterministic (time dependent) disturbing quantities. The theoretical investigation concentrated in particular on the effects from

- quantization of the input quantity (deflection) into "quantization intervals";
- filtering of the interferometer signal (e.g., low-pass and high-pass filter);
- electric noise (e.g., low-pass limited white noise);
- sinusoidal voltages (e.g., hum, high-frequency laser light intensity modulation);
- trigger hysteresis;
- disturbing phase shifts (variations in the optical path difference);
- disturbing motions of the measuring reflector (e.g., harmonics from nonlinear distortion of a vibration exciter, random vibration from ground motion);
- other error sources.

The term error of measurement is defined in the *International Vocabulary of Basic and General Terms in Metrology* (VIM, 1993) as the result of a measurement minus the true value of the measurand. In the context of error analysis which is the subject of this paper, as a conventional true value, that measurement result is used which would exist if there were no disturbing quantity (e.g., electric noise voltage). Treating an error as a random variable, its expected value as expressed in the following section is included as a systematic error, allowing the optimum measurement conditions to be recognized and if necessary, the result of measurement to be corrected. The error's variance (or standard deviation) characterizes an individual uncertainty among all those that have to be taken into account as possible contributions to the total measurement uncertainty (cf. the note in the introduction and the final section).

THEORETICAL ERROR DESCRIPTION

Error Due to Quantization

The following expression has been established by Von Martens and Täubner (1983) to describe the quantization error:

$$e_Q = \begin{cases} \Delta\hat{x} \quad \text{for} \\ \quad \mu\pi \leqslant \varphi_0 < (\mu + 1/2)\pi - 2\pi|\Delta\hat{x}|/\Delta x, \\ -\Delta\hat{x} + (\operatorname{sgn}\Delta\hat{x})\Delta x/4 \quad \text{for} \\ \quad (\mu + 1/2)\pi - 2\pi|\Delta\hat{x}|/\Delta x \leqslant \\ \qquad \varphi_0 < (\mu + 1/2)\pi + 2\pi|\Delta\hat{x}|/\Delta x, \\ \Delta\hat{x} \quad \text{for} \\ \quad (\mu + 1/2)\pi + 2\pi|\Delta\hat{x}|/\Delta x \leqslant \\ \qquad \varphi_0 < (\mu + 1)\pi, \end{cases} \tag{12}$$

where $\Delta\hat{x} = \hat{x} - \hat{x}_0$, $\hat{x}_0 = (2\nu + 1)\Delta x/4$,

$$\nu = \operatorname{int}\left(\frac{\hat{x}}{2\Delta x}\right),$$

and $\mu = 0, \pm 1, \pm 2, \ldots$. The probability calculus can be used to demonstrate that, under certain conditions, Eq. (11) remains valid down to small amplitudes $\hat{x} < \Delta x$. When the zero-phase angle φ_0 of Eq. (2) is considered a random variable with probability density $f_{\varphi_0}(\varphi_0)$, the interferometer signal given by Eq. (1) can be characterized by the joint distribution density $f_{u,\dot{u}}(u, \dot{u})$ between the voltage u and its derivative $\dot{u} = \mathrm{d}u/\mathrm{d}t$. The probability ΔF that a positive zero crossing occurs in a time interval $t_1 < t < t_1 + \Delta t$ can be expressed by the relation

$$\Delta F = \int_{u=u_T-\dot{u}\Delta t}^{u_T} \int_{\dot{u}=0}^{\infty} f_{u,\dot{u}}(u, \dot{u}; t_1)\mathrm{d}u\,\mathrm{d}\dot{u}, \tag{13}$$

where u_T is the trigger threshold voltage ($u_T \ll \hat{u}$). When the relation

$$f_{u,\dot{u}}(u, \dot{u}) = f_u(u) f_{\dot{u}}(\dot{u}), \tag{14}$$

with

$$f_u(u) = \frac{1}{\hat{u}\pi\sqrt{1 - \left(\frac{u}{\hat{u}}\right)^2}}, \tag{15}$$

$$f_{\dot{u}}(\dot{u}) = \frac{1}{\hat{\dot{u}}\pi\sqrt{1 - \left(\frac{\dot{u}}{\hat{\dot{u}}}\right)^2}}, \tag{16}$$

$$\hat{\dot{u}} = \frac{4\pi^2}{T_M}\left(\frac{\hat{x}}{\Delta x}\right)\hat{u}, \tag{17}$$

is introduced into Eq. (13), expression Eq. (11) is obtained when the integrals are solved and several conversions made. This relation is thus valid (largely) independently of the deflection amplitude $\hat{x}$ when the density functions Eqs. (15) and (16) are realized during the measurement to a sufficient approximation in the form of frequency distributions. In the case of a large amplitude, this condition is met practically when the interference fringes are counted over a single vibration period T_M. For a small amplitude (lower limit approximately $\hat{x} = 0.05\Delta x$), Eqs. (15)–(17) are approximately valid when, in the course of an integrating measurement over a sufficient number of vibration periods ($M \gg 1$), a constant frequency distribution (uniform distribution) of the zero-phase angle φ_0 is achieved within an interval

$$[\varphi_{01}; \varphi_{01} + m\pi], \quad m = 1, 2, \ldots . \tag{18}$$

If no disturbing zero-phase variations are present, this condition can be met by a modified counting method with linear zero-phase variation, as will be shown in the final section.

For measurement conditions in which disturbing zero-phase variations do occur, another version of the counting method with excitation of a stochastic zero-phase variation has been developed (cf. the final section). An added low-frequency narrow-band stochastic process with well-defined parameters dominates the disturbing variations and suppresses the quantization error when a suitable standard σ_{φ_0} is selected (cf. Fig. 1a and b) and the time of measurement is long enough.

To determine the time of measurement necessary, the autocorrelation function of the quantization error was derived for conditions of measurement which are of interest (cf. Fig. 2a and b). From the autocorrelation function the variance of the quantization error can be obtained as a function of the time of measurement using a relation presented by Davenport et al. (1952), cf. Fig. 3a and b.

Error Due to Filtering

A prerequisite for the accurate measurement of the motion characteristics based on the counting of the zero crossings is the linear transformation of the significant part of the interferometer signal's frequency spectrum. Transformation of the interferometer signal should be achieved with a frequency characteristic which is flat (constant) as regards the amplitude and linear as regards the phase. Another point of interest is the suppression of noise by appropriate filtering of the output voltage of the photoreceiver, including the signal conditioner. A high-pass frequency characteristic may be obtained if a special photoreceiver, is chosen (e.g., avalanche photodiode), or it may be additionally introduced to suppress flicker noise. Low-pass filtering is applied to suppress high-frequency noise. In order to find the optimum filter characteristics, the error due to filtering has been investigated.

The problem has been solved in the following steps. The interferometer output signal is expressed in terms of its Fourier series:

$$\begin{aligned} u(t)/\hat{u}_M = {} & \cos\varphi_0\left[J_0(\hat{\varphi}_M) - 2J_2(\hat{\varphi}_M)\cos 2\omega_M t \right. \\ & \left. + 2J_4(\hat{\varphi}_M)\cos 4\omega_M t - \cdots\right] \\ & - \sin\varphi_0\left[2J_1(\hat{\varphi}_M)\cos\omega_M t \right. \\ & \left. - 2J_3(\hat{\varphi}_M)\cos 3\omega_M t + \cdots\right], \end{aligned} \tag{19}$$

where the J_n are Bessel functions of the first kind, of order n. A number of filter types of different orders have been computer-simulated (for example the filter coefficients of Bessel and Butterworth filters, low and high passes, first to fourth order). The sinusoids have been added after having been multiplied with the amplitude frequency response, and phase-shifted with the phase frequency response of the filter at the frequencies $f_n = nf_M$, $n = 1, 2, \ldots$.

As an example, Fig. 4 shows an unfiltered and a filtered signal in a special case where a small deflection amplitude is applied. The zero crossings are calculated from the resulting filtered signal. A comparison between the measurement results obtained when the calculated zero crossings of the filtered and unfiltered signals are used leads to a relationship for the error due to filtering. Some examples showing the calculated relative measurement error due to low-pass filtering as a function of the normalized cut-off frequency are presented in Figs 5 and 6. An example demonstrating the calculated relative measurement error due high-pass filtering as a function of the normalized deflection amplitude is given in Fig. 7. The considerable error that may be caused by a high-pass characteristic (cf. Fig. 7) can basically be suppressed by frequency conversion as described by Von Martens (1993).

Error Due to Electric Noise

In general, electric noise can be suppressed by sufficient trigger hysteresis. If small deflection amplitudes are obtained by counting the zero crossings of the interferometer signal, some zero passes may not be identified if the hysteresis is relatively large. An investigation into the noise influence taking into account the trigger hysteresis is therefore of practical interest. The

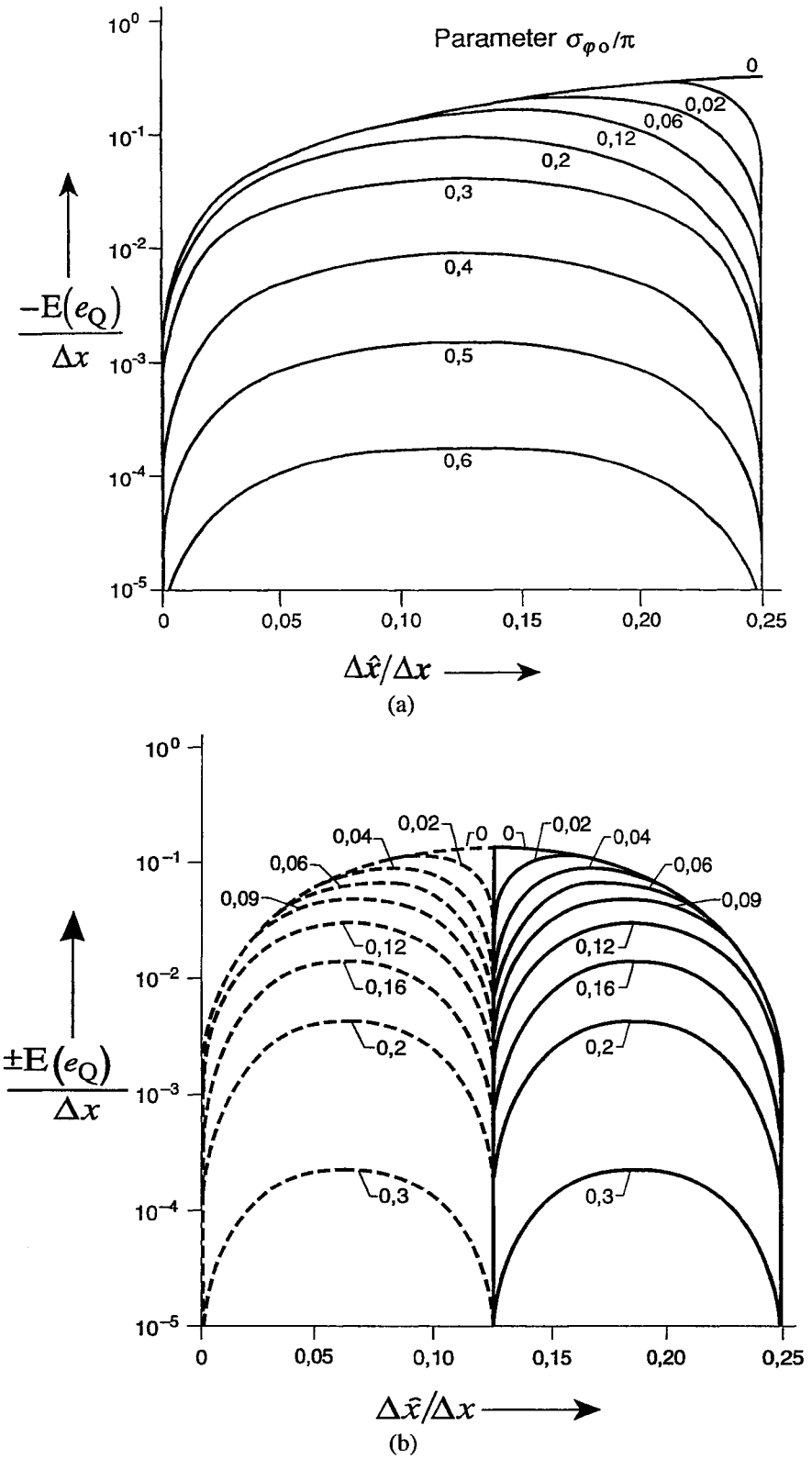

FIGURE 1 (a) Expected value of the quantization error as a function of the residual section $\Delta\hat{x}$ of the deflection amplitude $\hat{x}$. $\Delta\hat{x}$ defined by Eq. (12), zero-phase angle φ_0 is narrow band stochastic process of 2nd order with: resonance rise $Q = 10$, expected value $E(\varphi_0) = 0 + \mu\pi$, $\mu = 0, \pm 1, \pm 2, \ldots$, standard deviation $\sigma_{\varphi 0}$. (b) The same but with expected value $E(\varphi_0) = \pi/4 + \mu\pi$.

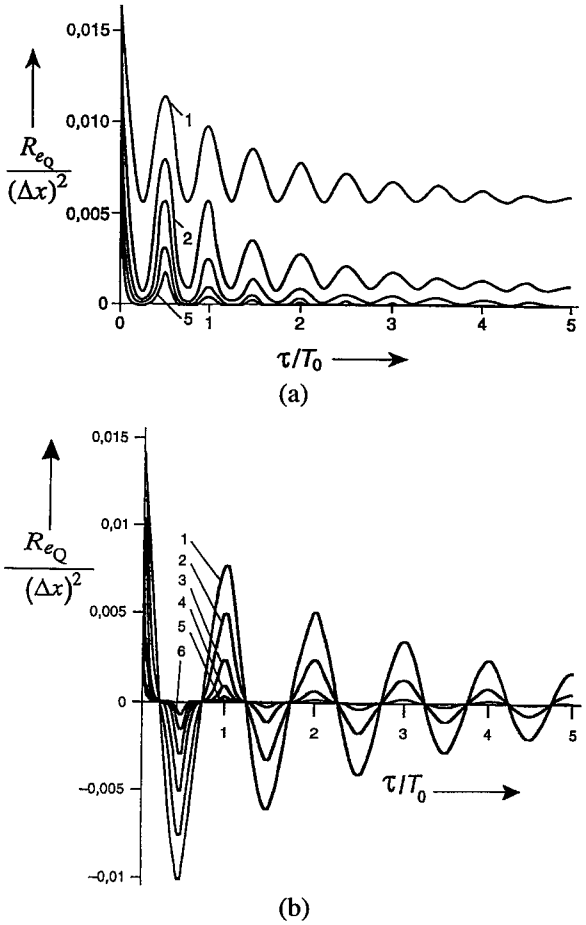

FIGURE 2 (a) Normalized autocorrelation function of the quantization error e_Q. As Fig. 1a but with $\hat{x} = \Delta x/8 + \nu\Delta x/4$; $\nu = 0, 1, 2, \ldots$, $\sigma_{\varphi 0} = 0.2\pi$ (curve 1), 0.3π (curve 2), ... , 0.6π (curve 5). (b) The same but with expected value $E(\varphi_0) = \pi/4 + \mu\pi$; curve 6: $\sigma_{\varphi 0} = 0.7\pi$.

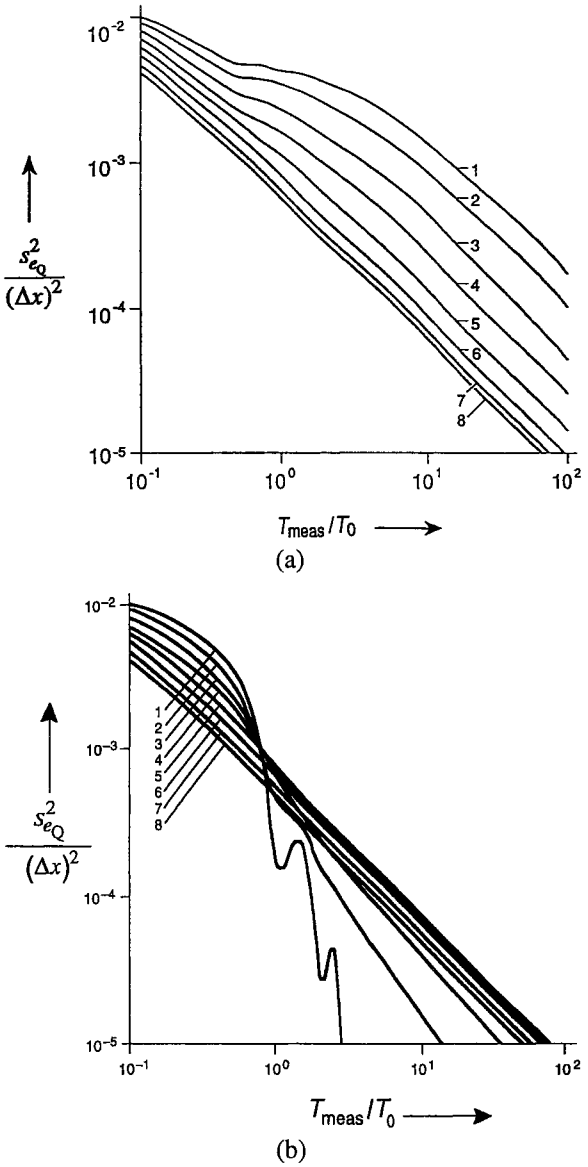

FIGURE 3 (a) Normalized variance of the quantization error e_Q as a function of the measurement integration time. As Fig. 2a but with $\sigma_{\varphi 0} = 0.3\pi$ (curve 1), ... , 1.0π (curve 8). (b) The same but with expected value $E(\varphi_0) = \pi/4 + \mu\pi$.

disturbing effect of the trigger hysteresis as regards missing impulses is described below.

Relationships describing the expected value and the variance of the error due to stochastic noise have been established for those ergodic stochastic processes for which the autocorrelation function and second derivative can be determined. The approach by Rice (1945, 1948) introduced to express the expected value of the zero crossings of noise and/or of a sinusoid with additive noise has been made use of. In contrast to the deterministic measurement signal formulation by Rice (1948), a statistical characterization of the measurement signal by the joint distribution density has been introduced by Von Martens (1993), allowing the expected value and the variance of the measurement error to be estimated as a function of the trigger hysteresis.

The expected value of the relative error e^*_N due to noise can be expressed by

$$E(e^*_N) = 8.4 \times 10^{-3} D_{N,E} (T_M f_{LP})^2 \left(\frac{\tilde{u}_N}{\hat{u}_M}\right)^2 \left(\frac{\Delta x}{\hat{x}}\right)^2, \tag{20}$$

and the variance by

$$s_{e^*_N} = 6.1 \times 10^{-4} D_{N,V} \frac{1}{M} (T_M f_{LP})^3 \left(\frac{\tilde{u}_N}{\hat{u}_M}\right)^2 \left(\frac{\Delta x}{\hat{x}}\right)^3, \tag{21}$$

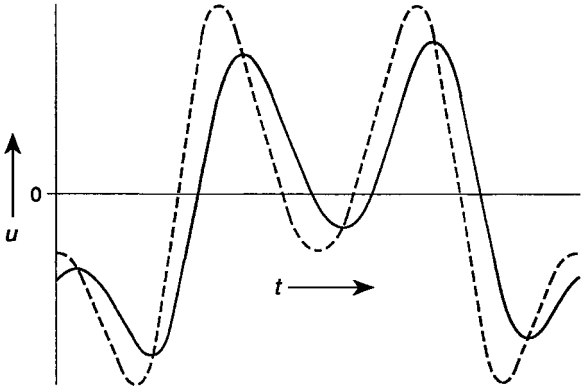

FIGURE 4 Demonstration of distortion influence of filtering on the interferometer signal $u(t)$. Sinusoidal motion quantity with deflection amplitude $\hat{x} = \Delta x/2$, interferometer signal zero phase angle $\varphi_0 = 2\pi/5$. Broken: unfiltered interferometer signal; solid: interferometer signal filtered by low-pass of 1st order.

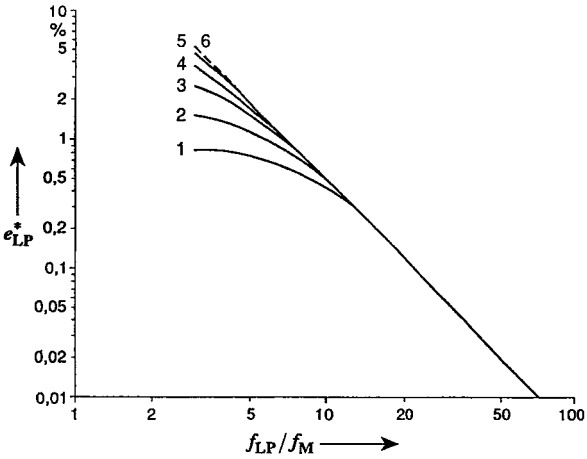

FIGURE 5 Relative error e^*_{LP} due to low-pass filtering (1st order filter) as a function of the normalized cut-off frequency f_{LP}/f_M. Sinusoidal motion quantity with frequency f_M and deflection amplitude $\hat{x}$. Parameter is the normalized amplitude $\hat{x}/\Delta x = \frac{1}{4}, \frac{1}{2}, 1, 2$, and 4 for curve 1, 2, 3, 4 and 5, respectively. Curve 6 shows a function proportional to $(f_{LP}/f_M)^{-2}$ as an approximation.

where T_M is the vibration period, f_{LP} the cut-off frequency of an assumed low-pass limited white noise, $\hat{u}_M$ the signal amplitude, $\tilde{u}_N$ the rms value of the noise voltage, and $D_{N,E}$, $D_{N,V}$ are "damping factors" that characterize the hysteresis influences on the expected value and on the variance, respectively (cf. Fig. 8). Similar relationships have been established for band-pass limited noise.

Error Due to Sinusoidal Voltages

Parasitic sinusoidal voltages that may occur in addition to the measurement signal can cause different disturbing effects depending on their frequencies, e.g., hum on the one hand, and a high-frequency sinusoid on the other. Only the effects of a high-frequency sinusoid are discussed in this section. In the presence of a sinusoidal voltage whose derivative exceeds the derivative of the measurement signal, repeated zero crossings may occur which lead to wrong counting impulses and thus to an error of measurement. Following the approach of characterizing the measurement signal by its joint distribution density which was introduced by Von Martens (1993) to estimate the random noise influences (cf. subsection above), relationships have been established allowing the expected value $E(e^*_S)$ and the second statistical moment m_{2,e^*_S} of the error due to the sinusoid to be estimated:

$$E(e^*_S) = 8.3 \times 10^{-3} D_{S,E} \left(\frac{T_M}{T_S}\right)^2 \left(\frac{\hat{u}_S}{\hat{u}_M}\right)^2 \left(\frac{\Delta x}{\hat{x}}\right)^2, \tag{22}$$

$$m_{2,e^*_S} = 2.7 \times 10^{-4} D_{S,m_2} \left(\frac{T_M}{T_S}\right)^4 \left(\frac{\hat{u}_S}{\hat{u}_M}\right)^3 \left(\frac{\Delta x}{\hat{x}}\right)^4. \tag{23}$$

$D_{S,E}$ and D_{S,m_2} are the "damping factors" characterizing the influence of the trigger hysteresis on the expected value, and the second statistical moment of the error due to a sinusoidal disturbing voltage (cf. Fig. 9); $\hat{u}_M$ is the signal amplitude and $\hat{u}_S$ the amplitude of the disturbing sinusoid.

The variance of the relative error of measurement can be obtained using the expression

$$s^2_{e^*_S} = \frac{1}{M}\left(m_{2,e^*_S} - E^2(e^*_S)\right). \tag{24}$$

It should be remembered that the statistical frequency distribution of the measurement signal is approximately realized by special means (cf. the final section).

Error Due to Trigger Hysteresis

It is possible at each turning point of the motion (displacement or rotation angle) that a zero crossing is not counted. A counting impulse will be missing if the interferometer signal, after having passed the trigger level in, say, a positive direction, thus releasing a counting impulse, changes the direction and crosses the trigger level in a negative direction, but without leaving the hysteresis zone before again exceeding the trigger level. A detailed description of the measurement error due to hysteresis has been presented by

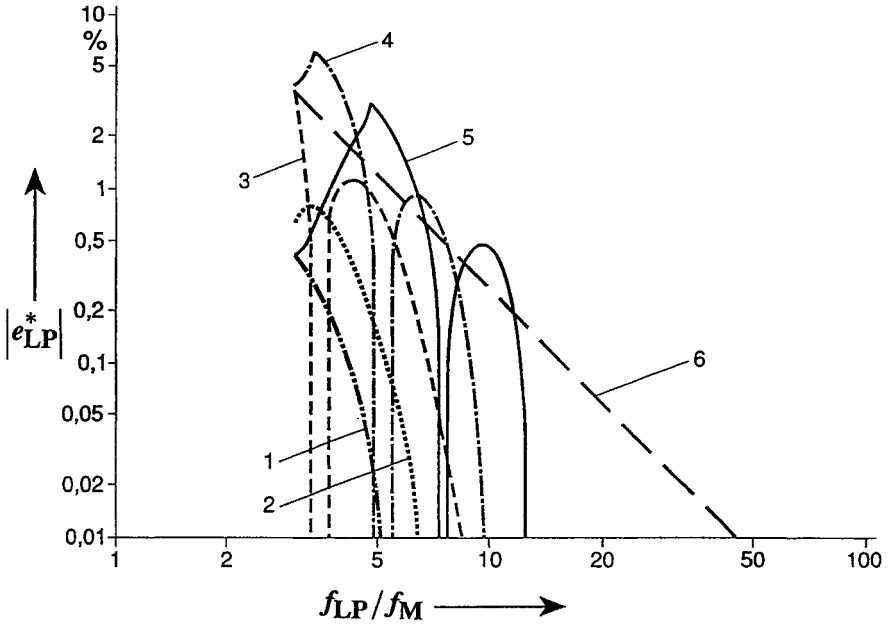

FIGURE 6 Magnitude of the relative error e^*_{LP} due to low-pass filtering (4th order filter) as a function of the normalized cut-off frequency f_{LP}/f_M. Sinusoidal motion quantity with frequency f_M and deflection amplitude $\hat{x}$. Parameter is the normalized amplitude $\hat{x}/\Delta x = \frac{1}{8}, \frac{1}{4}, \frac{1}{2}$, 1 and 2 for curve 1, 2, 3, 4 and 5. Curves 1 to 5 are valid for Butterworth low pass. Curve 6 is valid for Bessel low pass and covers all amplitudes stated above.

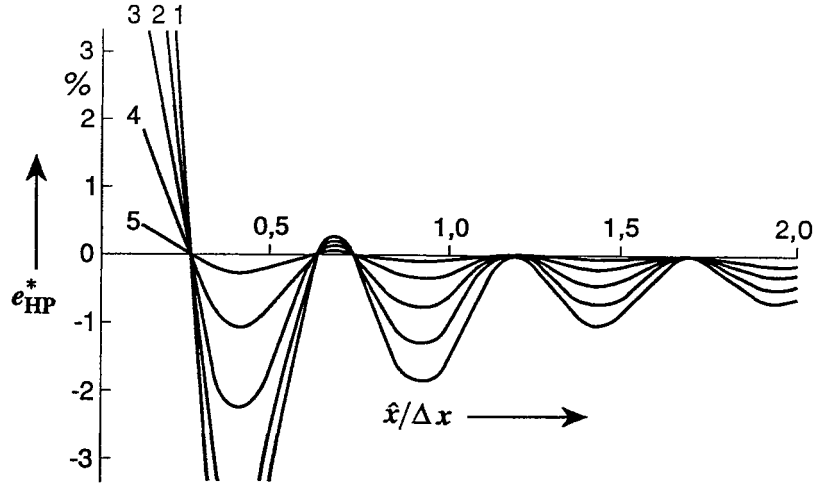

FIGURE 7 Relative error e^*_{HP} due to high-pass filtering (1st order filter) as a function of the normalized deflection amplitude $\hat{x}/\Delta x$ of a sinusoidal motion quantity with a frequency f_M. Parameter is the normalized cut-off frequency $f_{HP}/f_M = 0.1, 0.2, 0.3, 0.4$ and 0.5 for curve 1, 2, 3, 4 and 5, respectively.

Von Martens and Täubner (1983). During the integrating counting process over a large number of vibration periods, this error approaches its expected value, which can be treated as a systematic error. The error due to hysteresis can therefore be eliminated, to a certain degree, by correction of the measurement result. From the investigation described in the reference, the relationship for the expected value of this error,

$$\mathrm{E}(e^*_H) = -\frac{1}{4\pi}\frac{u_H}{\hat{u}_M}\frac{\Delta x}{\hat{x}}, \tag{25}$$

applies for the case which is of practical interest, i.e., where the hysteresis u_H and the trigger level u_T are small compared with the signal amplitude

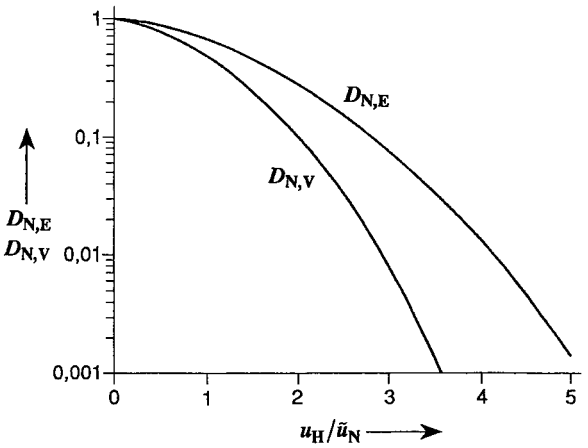

FIGURE 8 Damping rates of the relative error e_N^* due to electric noise as a function of the normalized trigger hysteresis (Eqs. (20), (21)). $D_{N,E}$ damping rate for expected value $E(e_N^*)$, $D_{N,V}$ damping rate for variance $s^2_{e_N^*}$, u_H trigger hysteresis, $\hat{u}_M$ signal amplitude, $\tilde{u}_N$ noise voltage rms value.

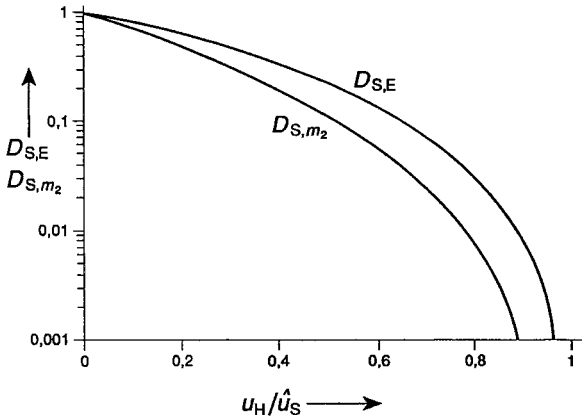

FIGURE 9 Damping rates of the relative error e_S^* due to sinusoidal disturbing voltage as a function of the normalized trigger hysteresis (Eqs. (22), (23)). $D_{S,E}$ damping rate for expected value $E(e_S^*)$, $D_{S,m2}$ damping rate for variance $s^2_{e_S^*}$, u_H trigger hysteresis, $\hat{u}_M$ signal amplitude, $\hat{u}_S$ amplitude of the disturbing sinusoid.

$\hat{u}_M$. The relative measurement error may assume too large a value if small displacement or rotation angle amplitudes are measured. As the relation $u_H/\hat{u}_M$, whose value is needed for correction, is generally not accurately known, it is useful to select a relatively small hysteresis. The relationships described by Eqs. (20)–(24) allow a hysteresis value to be estimated that is relatively small but sufficient to suppress electric noise and high-frequency sinusoidal voltages.

Error Due to Disturbing Motions and Phase Shifts

A variety of parasitic motions exists acting in addition to the measurand, which is assumed to be sinusoidal. If a nominally sinusoidal motion quantitiy is to be measured, its fundamental harmonic is considered the measurand, even if, as is usual, other harmonics are present, resulting from the nonlinear distortion of a vibration exciter. Other sources of disturbing motions may be, for example, hum from a power amplifier that feeds an electromechanical exciter, and stochastic ground motion. In principle, the effects of disturbing motions can be largely suppressed by using a special signal processing method that is based on an approximation of the pairs of measured deflection–time values using the least-squares method, with a sine to be approximated as is described by Von Martens and Täubner (1994). The error due to disturbing motion has been theoretically and experimentally investigated for different methods of signal processing. For the peak value measuring version (especially the fringe counting method), the following expressions have been established:

Relative measurement error due to odd harmonics:

$$e^*_{x_{S,2n-1}} = -k_x \cos\varphi_S + \frac{1}{4}(k_x q)^2(1 - \cos 2\varphi_S). \quad (26)$$

Relative measurement error due to even harmonics:

$$e^*_{x_{S,2n}} = \frac{1}{4}(k_x q)^2(1 + \cos 2\varphi_S). \quad (27)$$

Expected value of the relative measurement error if the disturbing motion shows an equally distributed phase angle or is not synchronized with the measurand:

$$E(e^*_{x_S}) = \frac{1}{4}(k_x q)^2. \quad (28)$$

In the relationships above, $k_x = \hat{x}_S/\hat{x}_M$, $q = f_S/f_M$ and φ_S is the phase angle difference between the disturbing and the measured sinusoids. In the case of nonsinusoidal disturbing motions, the following expressions apply:

Relative measurement error due to a constant drift velocity v_0:

$$e^*_{v_0} = \frac{1}{2}v_0^2/(\omega_M \hat{x}_M)^2. \quad (29)$$

Expected value of the relative measurement error due to stochastic motion

$$E(e^*_{\tilde{v}}) = \frac{1}{2}\tilde{v}^2/(\omega_M \hat{x}_M)^2, \quad (30)$$

where $\tilde{v}$ is the rms value of the velocity of a random vibration that is presupposed to be normally distributed.

Errors Due to Other Sources; Discussion

The errors described in the previous subsections characterize to a great extent the dynamic behaviour of a two-beam interferometer (including the diffraction grating interferometer) when the fringe counting method is applied to measure the amplitude of a sinusoidal motion quantitiy in the presence of disturbing motions, of additional phase variations in the interferometer signal and of electric noise. The approach made to assess the error of measurement should be applicable, to a great extent, irrespective of the particular design of the interferometric measurement system. For a given interferometer design and construction, further sources of errors may be significant, e.g., deviations from the ideal (sinusoidal) transfer characteristic between input deflection (displacement or rotation angle) and output voltage. However, a number of non-ideal properties of the interferometer (e.g., variations in the optical path difference or in the light intensity) can be expressed in the terms of such parasitic quantities of which the resulting errors are described by the formulas presented in the subsections above. A more detailed and comprehensive description covering other signal processing versions, too, is available.

APPLICATIONS AND CONCLUSIONS

The interferometric method described and analyzed in this article has been applied to six standard devices so far. Simplified block diagrams of four of them (e.g., low-, middle- and high-frequency acceleration standard, angular acceleration standard), Figs 10–13, are given to show in which way the special preconditions for suppressing the quantization error, formulated in previous section, have been technically realized.

At large displacement amplitudes such as those generated by the low-frequency acceleration standard (up to 0.5 m, cf. Fig. 10), the quantization error is negligible. The conventional counting method is therefore applied using a ratio counter. This method is used also by the angular acceleration standard (cf. Fig. 13) if large rotation angle amplitudes are to be measured.

In the middle frequency standard (cf. Fig. 11) two independed spring-suspended blocks isolate the exciter and interferometer from ground motion and avoid the pertubation of any optic element by the dynamic reaction forces from the exciter. The disturbing phase variations are dominated by a low-frequency narrow-band Gaussian noise added to the sinusoidal voltage at the input of the power amplifier which supplies the drive coil of the electrodynamic exciter.

In the high-frequency acceleration standard (cf. Fig. 12) any disturbing phase variations are suppressed, and the quantization error can thus be eliminated, by introducing a linear phase variation. Such a phase variation is excited by a ramp generator in conjunction with a piezoelectric translator. As a result, every spectral line of the frequency spectrum is split into two neighbouring spectral lines. With low-pass or narrow-band filtering, a beat signal (pure beat) is obtained whose zeros allow a variation of the zero-phase angle by 2π to be indicated and controlled.

The same approach to suppress the quantization error is applied to the standard device developed for circular motion quantities at sinusoidal time-dependences ("angular acceleration standard"). With non-sinusoidal time dependency (e.g., in the "shock acceleration standard", cf. Von Martens and Täubner (1994)) the quantization error is not relevant because the signal processing is based on the measurement of the time intervals between the zero crossings.

The above theoretical relationships between the disturbing quantities and the errors due to them have largely been experimentally confirmed. They can be used to select optimum conditions of measurement, eliminate systematic error components by corrections and estimate the measurement uncertainty. If the parameters (e.g., filter frequency limit or hysteresis) are not appropriately set, particular error components and thus, the relative error of measurement can easily run up to the order of 10%. By choosing the optimum conditions and applying the corrections as far as needed, error components have been kept as far below 0.1% as necessary to achieve this value as the measurement uncertainty in measurements of the amplitude of a sinusoidal motion quantity with low or no distortion. This relative "expanded uncertainty" of 0.1% was calculated according to the rules of the ISO Guide (1993) by combining the estimated variances (and co-variances) using the "root-sum-of-squares" method and multiplication of the "combined uncertainty" by the "coverage factor" $k = 2$.

In this way, in conjunction with the specially developed acceleration or angular acceleration exciters belonging to the above-mentioned standard devices, primary vibration calibrations of accelerometers and angular accelerometers are being carried out with a relative measurement uncertainty of 0.1 to 0.3% in the frequency range from 0.1 Hz to 10 kHz at the PTB. In primary shock calibrations, a minimum relative uncertainty of measurement of 0.5% has been achieved.

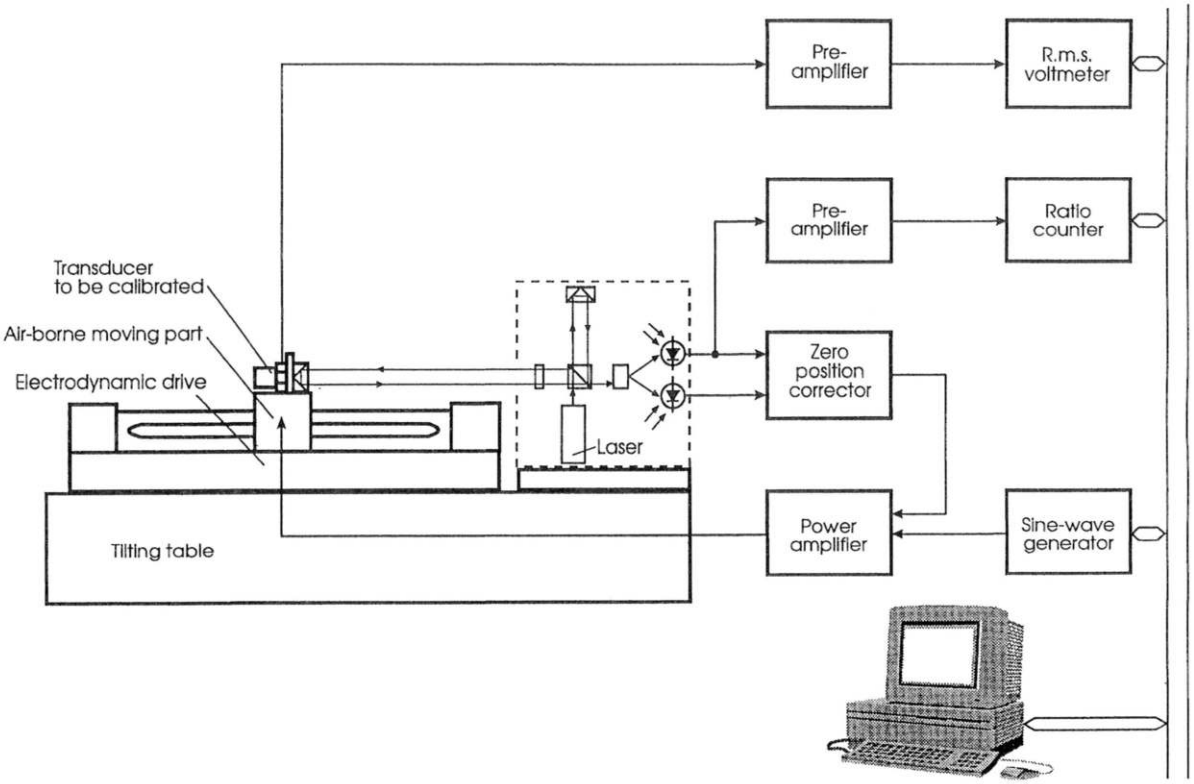

FIGURE 10 Simplified block diagram of low-frequency acceleration standard.

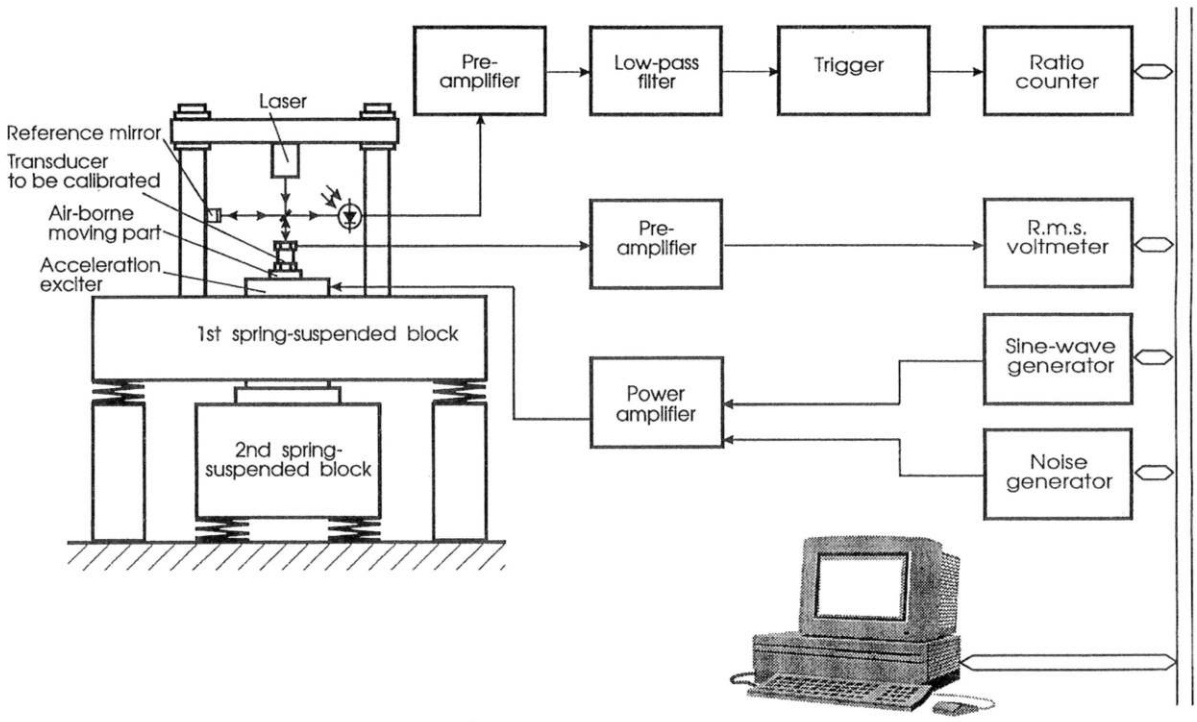

FIGURE 11 Simplified block diagram of middle-frequency acceleration standard.

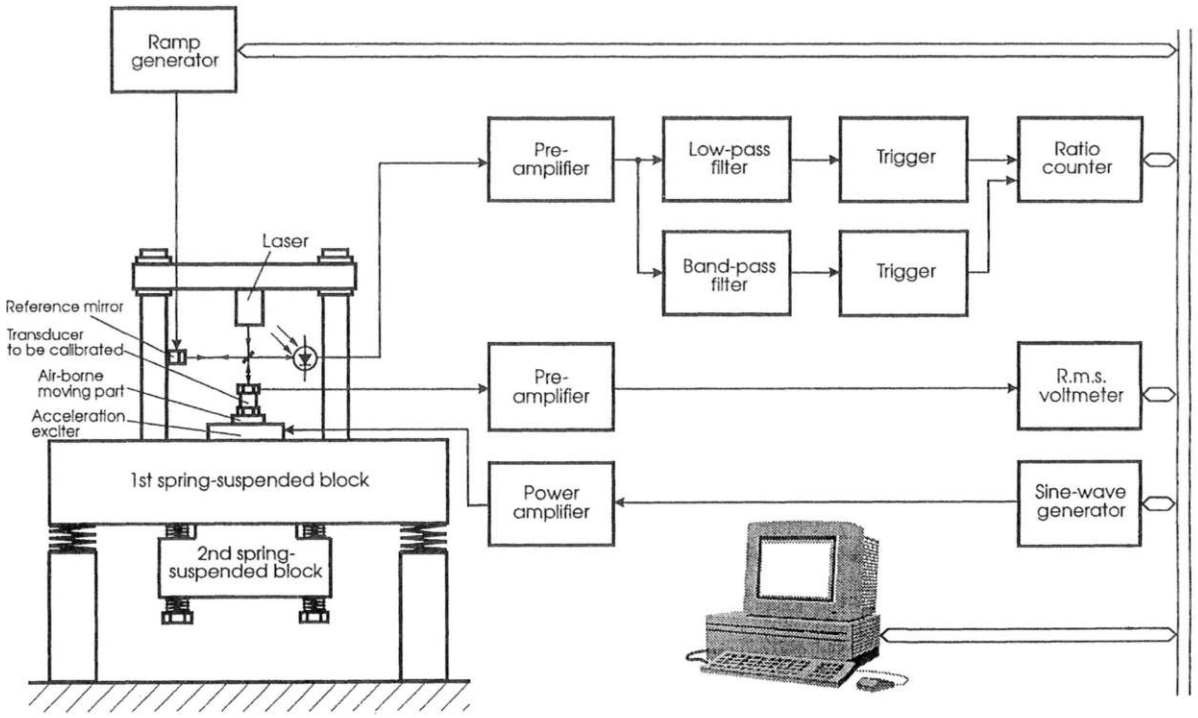

FIGURE 12 Simplified block diagram of high-frequency acceleration standard.

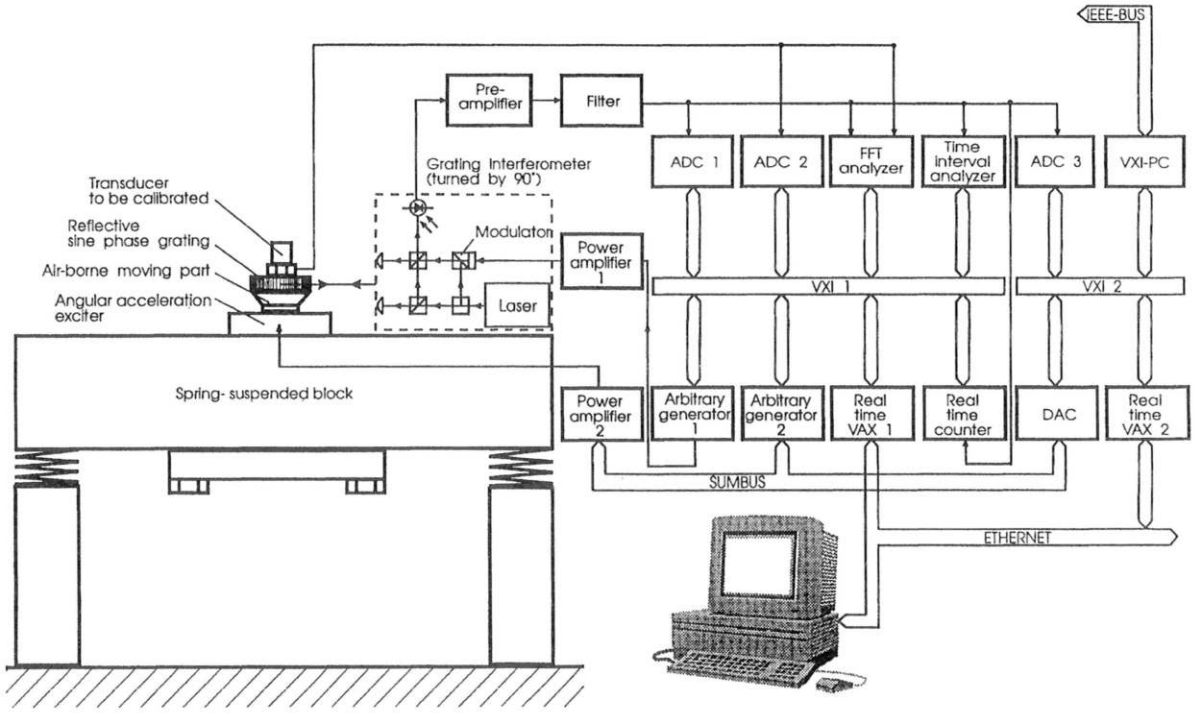

FIGURE 13 Simplified block diagram of angular acceleration standard.

REFERENCES

Davenport, W. B., Johnson, R. A., and Middleton, D., 1952, "Statistical errors in measurement on random time functions", *J. Appl. Phys.*, Vol. 23, pp. 377–388.

Harris, C. M., and Crede, Ch. E., 1987, *Shock and Vibration Handbook*, McGraw-Hill, New York, Toronto, London.

International Vocabulary of Basic and General Terms in Metrology, 1993, Genève, Switzerland.

ISO, Guide to the Expression of Uncertainty in Measurement, 1993, Genève, Switzerland.

ISO 5347-0, 1st edn., 1987, "Methods for the calibration of vibration and shock pick-ups", Part 0 "Basic concepts".

ISO 5347-1, 1st edn., 1993, "Methods for the calibration of vibration and shock pick-ups", Part 1 "Primary vibration calibration by laser interferometry".

Rice, S. O., 1945, "Mathematical analysis of random noise", *Bell Syst. Techn.*, 24, pp. 46–108.

Rice, S. O., 1948, "Statistical properties of a sine wave plus random noise", *Bell Syst. Techn.*, 27, pp. 109–157.

Serbyn, M. R., 1990, "Statistical analysis of an accelerometer round robin", *Report Nat. Inst. of Stand. and Techn.*, Gaithersburg.

Taylor, B. N., and Kuyatt, Ch. E., 1993, "Guidelines for Evaluating and Expressing the Uncertainty of NIST Measurement Results", *NIST Technical Note 1297.*

Von Martens, H.-J., 1987, "Interferometric counting methods for measuring displacements in the range 10^{-9} m to 1 m", *Metrologia*, Vol. 24, No. 4, pp. 163–170.

Von Martens, H.-J., 1993, "Dynamic calibration of rotational transducers by diffraction grating interferometry", *PTB-Mitteilungen*, Vol. 103, No. 1, pp. 19–26.

Von Martens, H.-J., and Rogazewski, P., 1987, "Representation and transfer of the units of vibration quantities in the GDR", *Bull. OIML*, Vol. 108, pp. 26–27.

Von Martens, H.-J., and Täubner, A., 1983, "On the theory of interferometric vibration measurements", (in German), *Metrologische Abhandlungen*, Vol. 3, No. 1, pp. 9–29.

Von Martens, H.-J., and Täubner, A., July 1994, "Interferometric measurement of translational and rotational motion quantities", *Proceedings* 10th International Conference on Experimental Mechanics, Lisboa, Portugal.